fire_cci

# D1.2.3 – Comprehensive Error Characterisation Report (CECR)

| | |
|---|---|
| **Project Name** | ESA CCI ECV Fire Disturbance (fire_cci) |
| **Contract N°** | 4000101779/10/I-NB |
| **Project Manager** | Arnd Berns-Silva |
| **Last Change Date** | 11/11/2014 |
| **Version** | 2.1 |
| **State** | Final |
| **Authors** | Marc Padilla, Emilio Chuvieco |
| **Document Ref:** | Fire_cci_Ph3_UAH_D1_2_3_CECR_v2_1 |
| **Document Type:** | Public |

Project Partners

| | |
|---|---|
| **Prime Contractor/ Scientific Lead** | – UAH - University of Alcalá de Henares (Spain) |
| **Project Management** | – GAF AG (Germany) |
| **System Engineering Partners** | – GMV - Aerospace & Defence (Spain)<br>– DLR - German Aerospace Centre (Germany) |
| **Earth Observation Partners** | – ISA - Instituto Superior de Agronomia (Portugal)<br>– UL - University of Leicester (United Kingdom)<br>– DLR - German Aerospace Centre (Germany) |
| **Climate Modelling Partners** | – IRD-CNRS - L'Institut de Recherche pour le Développement - Centre National de la Recherche Scientifique (France)<br>– JÜLICH - Forschungszentrum Jülich GmbH (Germany)<br>– LSCE - Laboratoire des Sciences du Climat et l'Environnement (France) |

# Distribution

| Affiliation | Name | Address | Copies |
|---|---|---|---|
| **ESA - ECSAT** | Stephen Plummer (ESA – ECSAT) | Stephen.Plummer@esa.int | electronic copy |
| **Project Team** | Emilio Chuvieco, (UAH)<br>Patricia Oliva (UAH)<br>Itziar Alonso (UAH)<br>Stijn Hantson (UAH)<br>Marc Padilla Parellada (UAH)<br>Arnd Berns-Silva(GAF)<br>Christopher Sandow (GAF)<br>Stefan Saradeth (GAF)<br>Federico González Alonso (INIA)<br>Jose Miguel Pereira (ISA)<br>Bernardo Mota (ISA)<br>Duarte Oom (ISA)<br>Gerardo López Saldaña<br>Kevin Tansey (UL)<br>Andrew Bradley (UL)<br>Luis Gutiérrez (GMV)<br>Ignacio García (GMV)<br>Andreas Müller (DLR)<br>Martin Bachmann (DLR)<br>Martin Habermeyer (DLR)<br>Kurt Guenther (DLR)<br>Thomas Krauß (DLR)<br>Eric Borg (DLR)<br>Martin Schultz (JÜLICH)<br>Angelika Heil (JÜLICH)<br>Florent Mouillot (IRD)<br>Julien Ruffault (IRD)<br>Philippe Ciais (LSCE)<br>Patricia Cadule (LSCE)<br>Chao Yue (LSCE) | Emilio.chuvieco@uah.es<br>patricia.olivap@gmail.com<br>itziar.alonsoc@uah.es<br>Hantson.stijn@gmail.com<br>padilla.marc@gmail.com<br>arnd.berns-silva@gaf.de<br>christopher.sandow@gaf.de<br>stefan.saradeth@gaf.de<br>alonso@inia.es<br>jmocpereira@gmail.com<br>bmota@isa.utl.pt<br>duarte.oom@isa.utl.pt<br>gerardoLopez@isa.utl.pt<br>kjt7@le.ac.uk<br>a.bradley@imperial.ac.uk<br>lgutierrez@gmv.com<br>igarcia@gmv.com<br>andreas.mueller@dlr.de<br>martin.bachmann@dlr.de<br>martin.habermeyer@dlr.de<br>kurt.guenther@dlr.de<br>thomas.krauss@dlr.de<br>eric.borg@dlr.de<br>m.schultz@fz-juelich.de<br>a.heil@fz-juelich.de<br>florent.mouillot@ird.fr<br>julien.ruff@gmail.com<br>philippe.ciais@cea.fr<br>patricia.cadule@lsce.ipsl.fr<br>chaoyuejoy@gmail.com | electronic copy on internal project website |

# Summary

This document is the Comprehensive Error Characterisation Report, and deals with the quality and error characteristics of the Burned Area (BA) product, as well as all intermediate information used to generate the final product, namely errors in the pre-processing of input data.

| | Affiliation/Function | Name | Date |
|---|---|---|---|
| **Prepared** | UAH | Marc Padilla, Emilio Chuvieco, | 04/08/2014, 07/10/2014 28/10/2014 |
| **Reviewed** | UAH | Emilio Chuvieco | 10/11/2014 |
| **Authorized** | UAH/ Prime Contractor | Emilio Chuvieco | |
| **Accepted** | ESA/ Project Manager | Stephen Plummer | |

# Signatures

| | Name | Date | Signature |
|---|---|---|---|
| **Signature of authorisation and overall approval** | Emilio Chuvieco | | |
| **Signature of acceptance by ESA** | Stephen Plummer | | |

# Document Status Sheet

| Issue | Date | Details |
|---|---|---|
| 1.0 | 04/08/2014 | First Document Issue |
| 2.1 | 28/10/2014 | Addressing ESA comments according CCI-FIRE-EOPS-MM-14-00xl.pdf |

# Document Change Record

| # | Date | Request | Location | Details |
|---|---|---|---|---|
| 2.1 | 11/11/2014 | UAH | Executive Summary | Indicating relevant products |
| | | | Section 1 | Updated and rephrased; |
| | | | Section 3.1 | Updated and rephrased; Indicating validation sites from 2006 – 2008; Table 1 updated; |
| | | | Section 3.2 | Updated and rephrased, Indication on final product; |
| | | | Section 3.2.2 | Introducing uncertainty assessment for the Grid Product; |
| | | | Section 3.3 | Updated; |
| | | | Section 4.1.1 | Restructured and updated; |
| | | | Section 4.1.2 | Updated; Introducing Figure 5 |
| | | | Section 4.2 | Updating Figure 6, Figure 7, Table 8, Table 9 |
| | | | Section 5.1 | Updated; |
| | | | Section 5.2 | Indication on pixel product; |
| | | | Section 6 | Updated; |
| | | GAF | Section 7 | Updated; |

# Table of Contents

# List of Tables



# List of Figures

# List of Abbreviations

| | |
|---|---|
| AATSR | Advanced Along-Track Scanning Radiometer |
| ABAMS | Automatic Burned Area Mapping Software |
| ATBD | Algorithm Theoretical Basis Document |
| BA | Burned Area |
| BIO | Biome |
| CCI | Climate Change Initiative |
| CECR | Comprehensive Error Characterisation Report |
| CL | Confidence Level |
| EBA | Estimated BA extent |
| ESA | European Space Agency |
| ECV | Essential Climate Variables |
| GAM | Generalized Additive Models |
| GFED | Global Fire Emissions Database |
| GLOBCOVER | ESA global land cover project |
| LC | Land Cover |
| MERIS | MEDium Resolution Imaging Spectrometer |
| MODIS | Moderate Resolution Imaging Spectroradiometer |
| NEI | Number of burned pixels in a 9x9 moving window |
| NGA | National Geospatial-Intelligence Agency |
| NSO | Number of valid daily observations |
| PB | Pixel actually burned |
| PSD | Product Specification Document |
| PVP | Product Validation Plan |
| RMSE | Root Mean Squared Error |
| SE | Standard Error |
| SLC | Scan Line Corrector |
| SZA | Solar Zenith Angle |
| TC | Tree Cover |
| VGT | CNES Earth’s observation sensor on-board SPOT-4 and SPOT-5 |

# Executive Summary

The Comprehensive Error Characterisation Report describes the methodology used to quantify the uncertainty of BA estimates of fire_cci Pixel and Grid Products, expressed in probabilistic terms, as required by end-users. Additionally, the effect of the main error sources has been assessed by means of regression analysis in the Products MERIS, VGT and MERGED.

# 1 Introduction

Error characterisation and validation are critical phases to generate any Essential Climate Variable (ECV), and therefore both have been included as key deliverables of the ESA CCI programme. While the validation gives information about the global quality of the product, the error characterisation tries to find out why those errors occur and under which conditions. An important practical output of the error characterisation in the fire_cci project is the uncertainty quantification of the Burned Area (BA) estimates, which is expressed in the uncertainty layer attached to the Pixel and Grid Products (see definition of both products in the PSD: Chuvieco et al. 2014).

The uncertainty is quantified commonly with the "general law of error propagation". As described in JCGM (2008a), the error is propagated from the input data to the product estimates through the functions used to derive the estimates. This functional based approach cannot, however, be used in the fire_cci project, given the dependence of the products on complex spatio-temporal functions and decision trees. Another approach deals with complex functions using Montecarlo simulations (Crosetto et al. 2001; Crosetto and Tarantola 2001; JCGM 2008b). The input error simulations are commonly very complex, as they must emulate the autocorrelations between errors, which may vary in time and space. Furthermore, the Montecarlo approach needs very large computational resources and the knowledge of the probabilistic distributions of the input data errors, not available in the fire_cci data, similarly as they are not available in other ECV products.

Another inductive approach based on validation data and regression analysis is also commonly used, and it will be the basis of our method. It has been commonly used for land cover maps. For example, Burnicki (2011) modelled through regression analysis the probability of misclassification of a land cover change map in Michigan (USA), and Smith et al. (2003) and van Oort et al. (2011) modelled the error of land cover maps to assess the effect of the landscape characteristics over the map category errors.

The antecedent works on uncertainty quantification for BA products are limited. Giglio et al. (2010) presented the BA uncertainty quantification used on the BA Global Fire Emissions Database version 3 (GFED3) product. The GFED3 product provides monthly BA extents at 0.5° spatial resolution based on the MODIS-MCD64 product, which gives the date of detection at 0.5 km spatial resolution derived from Moderate Resolution Imaging Spectroradiometer (MODIS) imagery coupled with MODIS active fire observations (Giglio et al. 2009). The uncertainty is expressed as a standard error of the BA extent estimated in the grid cell, and it is modelled with a linear regression of the burned patch residuals versus the actual extend of burned patches. In their study, the authors computed the per-patch residuals using reference data produced manually from Landsat imagery, at sample sites located in Siberia, Africa and North America.

Following the end-user requirements given during the project's progress meetings, the uncertainty of the fire_cci project will be estimated using a dedicated field in both the grid and pixel products. For the grid Product, uncertainty is expressed as a standard error of the total burned area for each grid cell, as requested by the CRG. This is a common practice in other ECVs, as it is in another global BA product, the GFED (Giglio et al., 2010). For the fire_cci Pixel Product, the uncertainty is expressed in probabilistic terms, as the probability that a pixel is really burned.

The analyses in the current deliverable have two main objectives:

- To quantify the uncertainty of BA estimates for the two final fire_cci products, Pixel Product and Grid Product.

- To characterise the main factors of error, so that it will be easier to understand why and in which conditions the errors tend to occur

The fire_cci reference data generated at the 10 Study Sites were used to measure the errors and regression analysis was used to assess the effect of error factors over the BA estimates.

# 2 Applicable and Reference Documents

| | |
|---|---|
| [AD-1] | ESA Climate Change Initiative (CCI) Phase 1, Scientific User Consultation and Detailed Specification, Statement of Work, EOP-SEP/SOW/0031-09/SP, v1.4, 2009 https://www.esa-fire-cci.org/webfm_send/110 |
| [AD-2] | ESA Climate Change Initiative. CCI Project Guidelines. Ref. EOP-DTEX-EOPS-SW-10-0002, issue 1, date of issue 05/11/2010. http://www.esa-fire-cci.org/webfm_send/117 |

# 3 Methods

## 3.1 Reference files

Errors were measured using reference data derived in the fire_cci project. These reference data were derived from multi-temporal pairs of Landsat images (30 m spatial resolution) following a protocol described in Padilla et al. (2011), which is adapted from the standard CEOS Cal-Val committee's guidelines. In the fire_cci project, reference data were generated yearly, from 1997 to 2009, with some exceptions due to cloud coverage and Landsat image availability. However, for the uncertainty characterisation of the fire_cci products, only validation sites from 2006 to 2008 (the time period with available data for fire_cci v3 of global products) were used. A total of 23 pairs of Landsat TM/ETM+ images were processed to generate these validation files (Table 1).

**Table 1: Number of image pairs used at the study sites.**

| Study site | #Image pairs | Study site | #Image pairs |
|---|---|---|---|
| Angola | 3 | Colombia | 3 |
| Australia | 3 | Kazakhstan | 1 |
| Borneo | 1 | Portugal | 3 |
| Brazil | 3 | Russia | 0 |
| Canada | 3 | South Africa | 3 |

Reference fire perimeters were co-registered and rescaled to the pixel size of the global BA products. Since Landsat-TM/ETM+ images have a much better spatial resolution than the global products, the comparison between the global and reference data was done by computing the proportion of each global pixel classified as burned in the reference pixels. Wherever global or reference data were not available (either because of cloud coverage or striping effects caused by the SLC-OFF problem of Landsat ETM+), those areas were labelled as non-observed and were discarded from further analysis. Only global product pixels with more than 66 % of observed area in the reference pixels were included in the analysis. This threshold restricted the analysis to the central part of SLC-OFF images.

## 3.2 Uncertainty assessment

### 3.2.1 Uncertainty assessment for the Pixel Product

The error characterisation was based on analysing the effect of four factors over the BA product accuracy:

1) The confidence level (CL):

This variable is generated by the BA algorithm when a particular pixel is detected as a burned pixel. CL is expressed using a fuzzy scale: the higher the value the higher the certainty of the BA estimate. No CL values are reported for the pixels classified as unburned. CL is expected to explain a large proportion of the error occurrences and low values of CL are expected to be associated with commission error.

2) The amount of available observations:

This factor is characterised by the number of valid daily observations (NSO), for the monthly period when the pixel is detected as burned. NSO is expected to be related with the error. Low values will indicate sparse observations because of cloud problems, and therefore likely errors in the fire detections and the dating. No NSO values are available for the pixels classified as unburned.

3) Burned patch size:

Small and fragmented fires are expected to be more difficult to detect as they will have more partially burned pixels, with less spectral contrast. Isolated pixels classified as burned or pixels belonging to an edge of an area classified as burned are likely to cover partially burned areas, and therefore a partial true burned classification or a partial commission error. This factor was characterised by computing the number of burned pixels in a 9 x 9 moving window (NEI), which range from 0 to 80. No NEI values are reported for the pixels classified as unburned. Pixels within a large area classified as burned, are less likely to be misclassified than the pixels located in the border of the area. Therefore, high values of NEI are expected to be associated with true burned classifications.

4) The land cover:

The spectral signatures of some land covers are similar to the signatures of the burned areas, which may produce commission errors. In addition, the spectral signature of fires over some land covers may persist for a short time period, causing consequently omission errors. This factor is characterised with three variables: the land cover (LC) obtained from the Globcover-2005 product, the biome (BIO), obtained from the Olson biomes (Olson et al. 2001b) and the percentage of tree cover (TC), obtained from the MODIS Vegetation Continuous Field Collection 5 (http://glcf.umd.edu/data/vcf/). Theoretically, the TC has a two-fold effect. On one hand, areas with high TC (e.g. dense forest) are expected to have a strong spectral contrast with a BA when crown fires occur, but on the other hand burns may be masked out in dense forest when fires only affect the understory, such as common in tropical regions and in Siberia. The categories for LC can be seen in Table 2 and for BIO in Table 3.

**Table 2: Acronyms for the land cover categories of the Globcover-2005 database**

| Globcover ID | Acronym | Full name of the land cover type |
|---|---|---|
| 11 | irrig.crop | Post-flooding or irrigated croplands (or aquatic) |
| 14 | rain.cropl | Rainfed croplands |
| 20 | agromosaic | Mosaic cropland (50-70%) / vegetation (grassland/shrubland/forest) (20-50%) |
| 30 | forestmosaic | Mosaic vegetation (grassland/shrubland/forest) (50-70%) / cropland (20-50%) |
| 40 | broad.everg. | Closed to open (>15%) broadleaved evergreen or semi-deciduous forest (>5m) |
| 50 | clos.decid. | Closed (>40%) broadleaved deciduous forest (>5m) |
| 60 | opendecid. | Open (15-40%) broadleaved deciduous forest/woodland (>5m) |

| Globcover ID | Acronym | Full name of the land cover type |
|---|---|---|
| 70 | clos.needl. | Closed (>40%) needleleaved evergreen forest (>5m) |
| 90 | openneedl. | Open (15-40%) needleleaved deciduous or evergreen forest (>5m) |
| 100 | mix.for | Closed to open (>15%) mixed broadleaved and needleleaved forest (>5m) |
| 110 | forest&grass | Mosaic forest or shrubland (50-70%) / grassland (20-50%) |
| 120 | grass&forest | Mosaic grassland (50-70%) / forest or shrubland (20-50%) |
| 130 | shrubland | Closed to open (>15%) (broadleaved or needleleaved, evergreen or deciduous) shrubland (<5m) |
| 140 | grass | Closed to open (>15%) herbaceous vegetation (grassland, savannas or lichens/mosses) |
| 150 | spar.veg. | Sparse (<15%) vegetation |
| 160 | reg.flodded | Closed to open (>15%) broadleaved forest regularly flooded (semi-permanently or temporarily) - Fresh or brackish water |
| 170 | mangroves | Closed (>40%) broadleaved forest or shrubland permanently flooded - Saline or brackish water |
| 180 | flooded | Closed to open (>15%) grassland or woody vegetation on regularly flooded or waterlogged soil - Fresh, brackish or saline water |
| 190 | urban | Artificial surfaces and associated areas (Urban areas >50%) |
| 200 | bare | Bare areas |
| 210 | water | Water bodies |
| 220 | snow | Permanent snow and ice |
| 230 | nodata | No data (burnt areas, clouds, etc.) |

**Table 3: Acronyms for the Olson biomes (Olson et al. 2001a)**

| Biome ID | Acronym | Biome full name |
|---|---|---|
| 1 | trop.moist.forest | Tropical and Subtropical Moist Broadleaf Forests |
| 2 | trop.dry.forest | Tropical and Subtropical Dry Broadleaf Forests |
| 3 | trop.conif.forest | Tropical and Subtropical Coniferous Forests |
| 4 | temp.broad.forest | Temperate Broadleaf and Mixed Forests |
| 5 | temp.conif.forest | Temperate Coniferous Forests |
| 6 | boreal.forest | Boreal Forests/Taiga |
| 7 | trop.savana | Tropical and subtropical grasslands, savannas, and shrublands |
| 8 | temp.savana | Temperate Grasslands, Savannas, and Shrublands |
| 9 | flooded.savana | Flooded Grasslands and Savannas |
| 10 | montane.savana | Montane Grasslands and Shrublands |
| 11 | tundra | Tundra |
| 12 | medit.forest | Mediterranean Forests, Woodlands, and Scrub |
| 13 | desert | Deserts and Xeric Shrublands |
| 14 | mangroves | Mangroves |
| 88 | lakes | Lakes |
| 99 | rock&ice | Rock and Ice |

A sample was selected from the data available at the ten Study Sites (SSs) of the fire_cci project. Since the regression analyses would require huge computational resources if the whole data available were processed, the sample was limited to 2 x $10^5$ pixels (around the 5 % of the sample available). These pixels are at the same spatial resolution of the global BA product, which is 300 m. A sample of 8700 pixels were randomly selected for each one of the 23 study sites/years with data available. Uncertainty quantification models were calibrated with 80 % of the observations of the randomly selected sample, and the remaining 20 % were used for an independent validation of the uncertainty estimates.

One of the main purposes of the analysis of the error factor effects was to define a model that properly estimates the product uncertainties, expressed as the probability that a pixel is actually burned ($Prob_{PB}$). The choice of the regression model was driven by the need of an uncertainty prediction method with low computer time requirements, so that it could be implemented in the fire_cci processing chain. The logistic model was the best according the computational efficiency criteria and allowed $Prob_{PB}$ to be modelled as function of the set of error factors:

$$\mathrm{Prob}_{PB,i} = \frac{1}{1+e^{-Z_i}} \quad (1)$$

with $Z_i$ being a linear function of the explanatory variables:

$$Z_i = \hat{\beta}_0 + \sum_{j=1}^{k} \hat{\beta}_j \mathrm{X}_{ij} \quad (2)$$

where $X_{ij}$ are the $k$ explanatory variables and $\beta_0$, $\beta_1$, $\beta_2$,…, $\beta_k$ are the $k$+1 parameters to be estimated through maximum likelihood methods. A pixel of the target product was considered as actually burned (PB) when it had more burned than unburned area in the reference data. The majority rule is the most common criterion for error modelling studies in land cover category maps (Burnicki 2011; Smith et al. 2003; van Oort et al. 2011).

Since the variables related to the product estimates (i.e. CL, NEI and NSO) are not available for unburned estimates, a model was defined and calibrated for the pixels estimated as burned and another one for the unburned estimates. The model for the uncertainty quantification of the BA product estimates was defined based on the variable performance and availability. A variable was selected only if it showed a significant effect on the single model or on the final uncertainty model. The uncertainty quantification model for the product pixels classified as burned had four eligible variables: CL, NSO, NEI and LC. One variable was eligible for the model for the pixels classified as unburned, LC.

Originally, the Merged Product was supposed to be the Pixel Product, the one to be delivered to end-users, and the variable selection was applied to that product. The selected variables were used as well for the MERIS and VGT products. Finally, a decision based on the accuracy of the products, established the MERIS Product as the final and only one. The current deliverable does not include the details of the variable selection of the MERIS product, as the uncertainty model was originally defined for the MERGED product. In any case, the uncertainty model was calibrated of course with the MERIS data, therefore the analysis is still valid, although, potentially, a better model could be defined for the specific case of MERIS.

The evaluation of the uncertainty quantification was based on the comparison between $Prob_{PB}$ and PB, in the independent dataset not used in the calibration of the uncertainty models. In the ideal case, almost all pixels with a $Prob_{PB}$ close to one should be actually burned, almost all pixels with a $Prob_{PB}$ close to zero should be actually unburned, and about half of the pixels with $Prob_{PB}$ close to 0.5 should be actually burned. To assess this relation, the proportion of PB was computed across the scale of $Prob_{PB}$, from 0 to 1 in segments of 0.1.

### 3.2.2 Uncertainty assessment for the Grid Product

The sample consisted on all the data available in the 23 study sites/years. Due to the large size of the 0.5° Grid Product cells, the whole size of the sample available in the sampled sites (64 observations) could be processed in a reasonable computing time. Similarly to the Pixel Product, the uncertainty quantification model was calibrated with the 80 % of the observations of the sample, randomly selected, and the remaining 20 % was separated for an independent validation of the uncertainty estimates.

The uncertainty of the Grid Product was expressed as the standard error (SE) of the estimated BA extent (EBA) by the product in each grid cell *i*. Similarly as in Giglio et al. (2010), standard error was modelled based on the error observed, according the reference data, and the product BA estimates as the explicative variable. Given that the Grid Product provides BA extents in 15-day periods, EBA values were computed from the Pixel Product to make sure an appropriate comparison with the BA extent of the reference data. The time periods with reference data were defined by the Landsat image pairs acquisition dates. The projected extent in earth surface of the Grid Product cells varies with the latitude, due to its coordinate system (Geographical Coordinates). Therefore, the uncertainty model was defined to predict SE based on EBA in terms of proportion of the grid cell (SEp and EBAp). Given a last requirement of end-users, the linear equation was designed without intercept, to make sure uncertainty is zero when no-burned area is estimated:

$$\hat{SEp}_i = \hat{\beta}_1 EBAp \tag{3}$$

where $\beta_1$ is a parameters estimated through maximum likelihood methods at the calibration sample. A standard error value, by definition has no a specific sign, therefore the observations of SEp were obtained, for each grid cell *i* of the sample, from the absolute value of the difference between EBAp and the observed BA proportion (BAp) from the reference data.

$$SEp_i = \mid EBAp_i - BAp_i \mid \tag{4}$$

Estimates of SEp were validated on the independent sample, not used in the calibration. According the Gaussian distribution theory, the intervals defined by EBAp ± $\hat{SEp}$ are expected to include around the 68.2% of the times the observed BAp, and this is what was evaluated in the independent sample.

The disagreement between EBAp and BAp was assessed over each pixel *i* on the whole data available in the 10 study sites, by means of root mean square error (RMSE), absolute bias (Bias) and relative bias (rBias), and additionally by the slope and coefficient of determination ($R^2$) of a linear regression analysis.

$$RMSE = \sqrt{\frac{\sum_{i=1}^{n}(EBAp_i - BAp_i)^2}{n}} \tag{5}$$

The bias of BA is measured as recommended in the CCI Project Guidelines (ESA 2010):

$$Bias = \frac{\sum_{i=1}^{n}(EBAp_i - BAp_i)}{n} \tag{6}$$

and in terms of relative bias (rBias), bias is standardized the amount of BA is actually burned:

$$rBias = \frac{\sum_{i=1}^{n} EBAp_i - BAp_i}{\sum_{i=1}^{n} BAp_i} \tag{7}$$

## 3.3 Error characterisation

Errors were characterised with regression models, in the same way as uncertainty was modelled, and using the same explanatory variables: number of neighbour pixels estimated as burned (NEI), confidence level (CL), number of sensor observations (NSO), tree cover density (TC), biome (BIO) and land cover (LC) (see section 2.2.1). The same data as Section 2.1 were used here.

The effect of a given variable on each error type, i.e. commission and omission of the burned area category, was assessed with Generalised Additive Models (GAM) which allows for non-linear effects between the response variable and covariates (Hastie and Tibshirani 1990). GAM is a Generalised Linear Model (GLM) with a linear predictor involving a sum of smooth functions of covariates (Wood 2006). The effect of the categorical variables was assessed through GLM.

The effect of the variables was explored by modelling each error type, with one explanatory variable at a time. The variable effects on the commission error were assessed by modelling the probability of a pixel with a commission error (PC), given the pixel was classified as burned by the product (PCB).

$$\text{Prob}\{\text{PC} \mid \text{PCB}\} = \frac{1}{1+e^{-\theta}} \tag{8}$$

with $\Theta$ being a smooth function of one variable at a time, calibrated through GAM. The variable effects on the omission error were assessed by modelling the probability of a pixel with an omission error (PO), given the pixel was actually burned (PB), i.e. with more burned than unburned area in the reference data.

$$\text{Prob}\{\text{PO} \mid \text{PB}\} = \frac{1}{1+e^{-\theta}} \tag{9}$$

The effect of the variables related to the product (NEI, CL and NSO) was not assessed as no values are available for the pixels classified as unburned, and therefore are not available for all observations of the dataset used to calibrate the regression models.

# 4 Results

## 4.1 Uncertainty assessment

### 4.1.1 Uncertainty assessment for the Pixel Product

The variable selected for the uncertainty quantification model was NEI, as being the only one with significant effect and available in the Merged Product. The $R^2$ of the uncertainty model was 0.127, and its coefficients are detailed in Table 4. Even the fairly low $R^2$ the model remains still valid, as it allows computing averages of uncertainty. Estimated uncertainties are expected vary little along the NEI range and at the worst case it would express simply an averaged of the uncertainty. Multiple regression models could potentially increase the explained variability in case information for other key error factors was available.

Given the low performance of the variables to explain the error at the pixels classified as unburned, the $Prob_{PB}$ was computed as a ratio, as the proportion of product pixels actually burned from the pixels classified as unburned by the product, which was 0.02. Following a last specific requirement of end-users the uncertainty for pixels classified as unburned was set to zero. Equations to compute uncertainty, the Layer 3 of the Pixel Product were the following:

If pixel is classified as burned $\Pr ob_{PB} = \frac{1}{1+e^{-(0.01\times NEI-0.39)}} \times 100$

If pixel is classified as unburned $\Pr ob_{PB} = 0$

**Table 4: The coefficients of the uncertainty quantification model for the burned classifications of the MERIS product. P-value refers to the significance of the coefficient difference to zero**

| | Coefficient | P-value |
|---|---|---|
| (Intercept) | -0.39 | 2.15e-04 |
| NEI | 0.01 | 6.57e-08 |

Figure 1 shows the scatter plot between the product uncertainty estimates ($Prob_{PB}$) and the binary classifications according to the reference data (1 if burned, and 0 if unburned), at the independent dataset not included in the model calibration. The black horizontal lines are formed by dots representing the pixels actually burned (PB; top) and unburned (down). As can be seen, there is a great vertical overlap in the two black dotted lines. Given that is difficult to appreciate the scatter of the dots, the blue segments have been designed to represent the proportion of PB for each range of $Prob_{PB}$ defined by the blue segment (from 0 to 1, by 0.1). As can be seen, there is approximately a one to one linear relationship between the $Prob_{PB}$ segments and the proportions of PB.

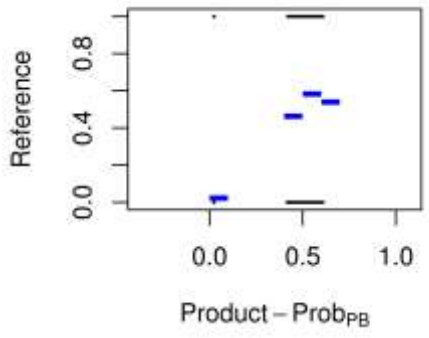


**Figure 1: Scatter plot between the product uncertainty estimates (ProbPB) and the reference binary classifications, 1 if burned (PB) and 0 if unburned, as the independent sample. Blue segments represent the proportion of pixels actually burned (PB) for each 0.1 range of ProbPB.**

### 4.1.2 Uncertainty assessment for the Grid Product

The $R^2$ for the estimated regression line was 0.136, its coefficients are detailed in Table 5 and the equation used to compute the standard error is as follows:

$$\hat{S}Ep = 0.38 \times EBAp$$

The coefficients of the uncertainty quantification equation for the Merged grid product are reported in Annex A.

**Table 5: The coefficients of the uncertainty quantification model for the Grid product. P-value refers to the significance of the coefficient difference to zero.**

| | Coefficient | P-value |
|---|---|---|
| EBAp | 0.38 | 0.001 |

Estimated SEp on the independent sample can be seen in Figure 2. The dots represent 0.5 degree grid cells located according to the BA proportion observed in the reference data (BAp; x-axis) and the estimated BA proportion according to the Grid Product (EBAp; y-axis). The vertical bars represent the intervals defined by the standard error (SEp) for each EBAp. The segments that cross the one to one line (in blue), show the product estimates that include the true value within one standard errors interval. In the independent sample, 25 % of the true BAp fell within the intervals defined by EBAp ± $\hat{S}Ep$ .

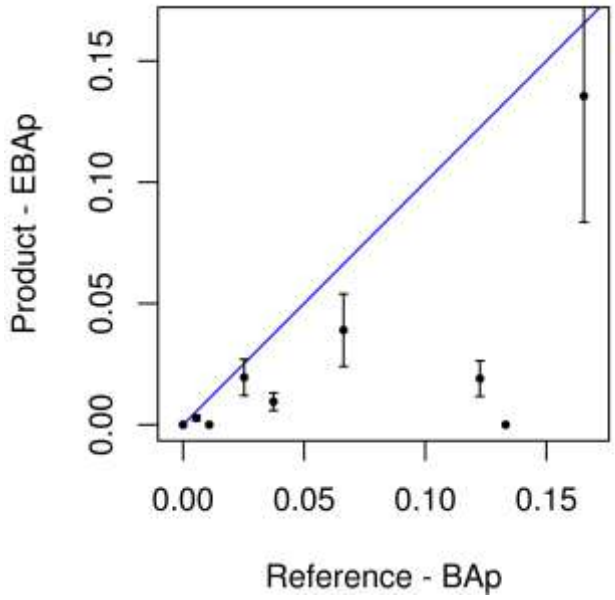


**Figure 2: BA estimates of the Grid Product (EBAp; y-axis), observed BA proportions (BAp; x-axis) and estimated uncertainties expressed as standard errors (SEp – vertical segments) in the independent sample. Blue line: 1:1 line.**

The RMSE of the Grid product BA estimates was 0.035, the Bias -0.015 and the rBias -0.59. Following the sign of the bias measures, BA is generally underestimated. Figure 3 shows the estimated regression line (slope = 0.41, intercept = -0.0002) between EBAp and BAp, for which the $R^2$ was 0.45. Given that linear regression may be affected by skewed distributions, the non-parametric Spearman $R^2$ is also computed: 0.59.

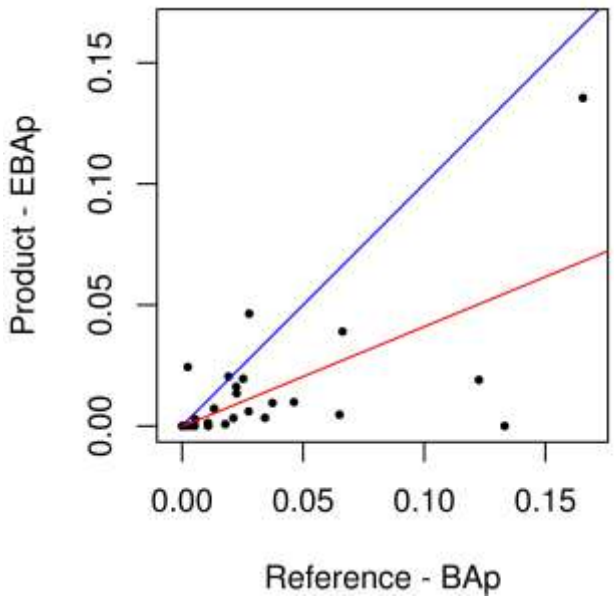


**Figure 3: BA estimates of the Grid Product (EBAp; y-axis), observed BA proportions (BAp; x-axis) for the whole sample (102 study sites/years), the estimated regression line (in red) and the 1:1 line (blue).**

## 4.2 Error characterisation

The effect of each variable on the commission errors of the MERIS Product is shown in Figure 4 for the quantitative variables and in Table 6 for the categorical variables. Similarly, the variable effects over the omission errors are shown in Figure 5 and Table 7. The detailed results for the Merged and VGT Products are reported in the Annex B. Each x-axis of the figures represents an explicative variable and the y-axes the probability of error predicted through GAM. The scatter plots between each variable and the errors (y-axis; 1 if error (commission or omission), and 0 if no-error) are also included in the figures. The black horizontal lines are formed by dots representing the pixels with errors, on the top of the figures, and the pixels with no-errors, on the bottom. As can be seen, there is a great vertical overlap between the two black dotted lines.

Particularly for the commission errors of the MERIS Product, TC and NSO had the strongest effects, as they had the highest $R^2$ (0.288 and 0.2 respectively), while NEI (0.021) and CL (0.006) had quite low. The fitted curves tend to show flat slope (lack of relationship) for NEI, a cyclic one for NSO and a curvilinear one for TC, which implies than commission errors tend to be higher for intermediate values of TC, being low for dense and sparse tree cover.

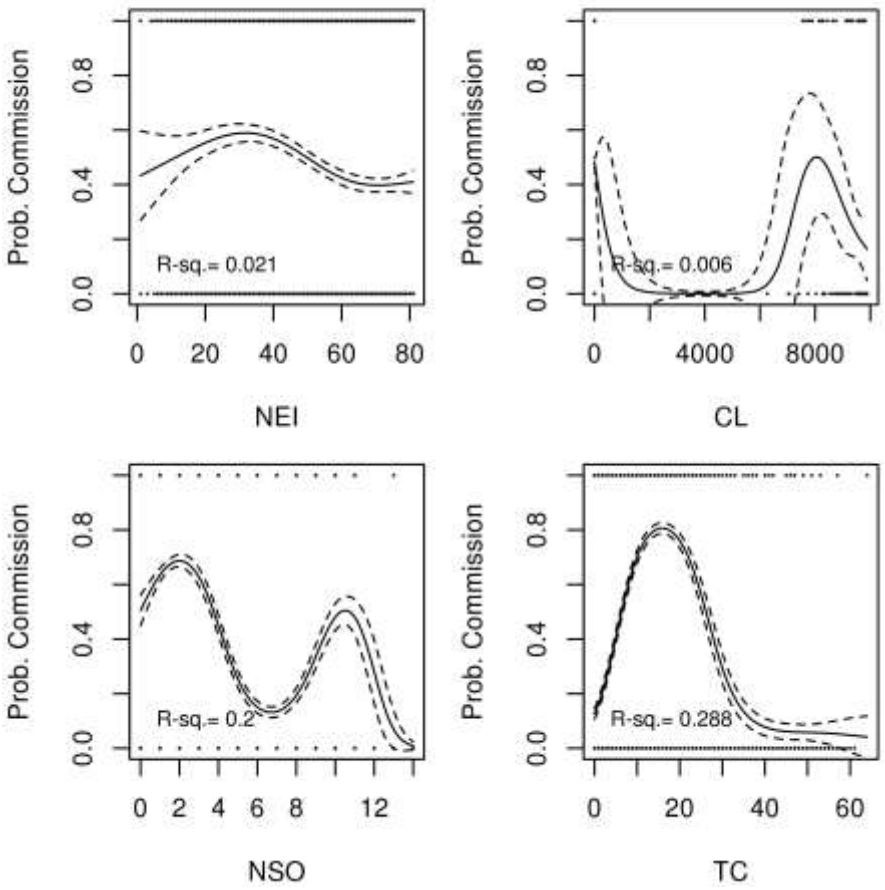


**Figure 4: Scatter plots between the explanatory variables (x-axes) and the commission errors (y-axes; 1 if error and 0 if no-error) for the intermediate product of MERIS. The relationship between each variable and the errors, calibrated through GAM, are shown with the expected probability of a commission error (solid line) and its 95% confidence intervals (slashed line). The coefficient of determinations (R-sq.) of each model, adjusted by the residual degrees of freedom, is shown at the bottom-right of the figures.**

**Table 6: Effects of the categorical variables over the commission errors of the MERIS Product. Nagelkerke R2 for the logistic regression models the sign of the coefficient in cases they are significantly different than zero ($\alpha < 0.05$).**

| Variable | Nagelkerke R2 | Signs of the coefficients with significant effect |
|---|---|---|
| BIO | 0.360 | boreal.forest(-); desert(-); temp.savana(+); trop.moist.forest(+); trop.savana(+) |
| LC | 0.395 | clos.needl.(-); forest& grass(+); grass(+); openneedl.(-); spar.veg.(-) |

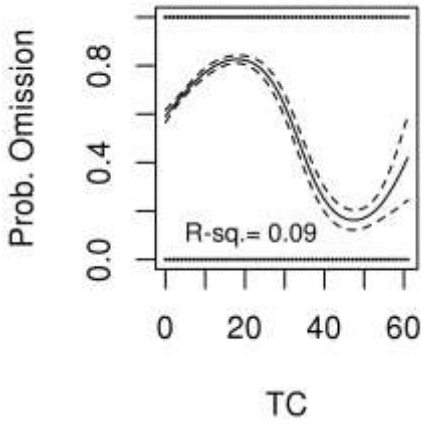


**Figure 5: As in Figure 4 but for the omission errors**

**Table 7: As in Table 6 but for the omission errors**

| Variable | Nagelkerke.R.square | Coeficient signs |
|---|---|---|
| BIO | 0.171 | boreal.forest(-); desert(+); medit.forest(+); temp.savana(-); trop.moist.forest(+); trop.savana(+) |
| LC | 0.138 | agromosaic(+); clos.needl.(-); forestmosaic(-); opendecid.(+); openneedl.(-); shrubland(+); spar.veg.(-) |

# 5 Discussion

## 5.1 Uncertainty assessment

The significant positive sign of NEI evidences that when a pixel classified as burned is located near the core of a burned patch the probability of being actually burned increases, while it decreases when is close to the edges. Assuming that the classification of the product reflects, at least in some degree, the actual burned patches, i.e. the product is not completely wrong, this evidence agrees with the conclusions found in antecedent works: the accuracy of thematic maps is higher in homogenous landscapes (Smith et al. 2003; van Oort et al. 2004), and particularly for BA maps the accuracy is higher where BA patches are more compact (Laris 2005; Sá et al. 2007; Silva et al. 2005).

The evaluation of the uncertainty quantification, based on NEI and expressed with the $Prob_{PB}$ values, showed that there are many actually burned pixels with low $Prob_{PB}$ values and many actually unburned pixels with high $Prob_{PB}$ values, as can be seen with the vertical overlap in the two black dotted lines in Figure 1. This reflects a limited performance of the uncertainty quantification when it is compared with the reference data. This is probably mainly due to a lack of performance in the uncertainty models, and may also be caused by an error factor not included in the analysis or simply by a randomness of the errors. This limited performance is also shown in the distribution of $Prob_{PB}$ values, there are not pixels with $Prob_{PB}$ between 0.02 and 0.4, and all of them above 0.02 are between 0.4 and 0.6. However, $Prob_{PB}$ may still be useful given that there are very few pixels with low $Prob_{PB}$ is actually true burned and that around half of the pixels with $Prob_{PB}$ close to 0.5 are actually true burned.

The uncertainty model for the Grid Product reflects, based only on EBAp shows that the expected error on BA extent is proportional to the estimated BA. The relatively low $R^2$ reflects the limited performance of the model. The standard errors are underestimated given that only the 25% of the true values fell within the intervals defined by EBAp ± $\hat{S}Ep$ (expected to be 68.2%). It is important to remember the small amount of data available (three years at the study sites).

The underestimation of the MERIS Grid Product agrees with the validation results of the MERIS Pixel Product reported in the PVR II (Padilla et al. 2014). The remarkable difference between the very low RMSE and the moderate $R^2$, suggesting very high and moderate accuracy respectively, may be caused by a biased distribution of EBAp and BAp values. The vast majority of 0.5 degree cells have low values of both estimated and observed BA proportions (i.e. low EBAp and Bap values, see points located at the origin axes in Figure 3), which implies a small RMSE.

The relatively low performance of the uncertainty models, for both MERIS Pixel and Grid products, suggests that other factors may also play important roles on the uncertainty. Particularly for the Grid product, further research may focus on the spatial distribution of the BA estimates, as similarly as in the Pixel product it may play an important role. Another relevant improvement could be to include in the current study the usage of a sample collected throughout a probability sampling design, instead the 10 study sites purposely selected currently used.

Currently the definition and calibration of the uncertainty models is done outside the processing chain. The inclusion of the uncertainty calibration and quantification within the processing chain would make sure an appropriate uncertainty model definitions and calibrations, even when new algorithm versions are released and no extra time is available for validation and error characterisation.

## 5.2 Error characterisation of the pixel product

The scatter plots between the variables and the errors show a great overlap in the two black dotted lines, which reflects the inability of some variables do discriminate between correctly and badly classified pixels. This inability is translated to the low $R^2$ scores and flat slopes on some regression models, particularly for NSO, and TC.

Similarly as in the uncertainty assessment, pixels located within compacted BA patches tend to have lower commission errors, commonly for all Products but particularly for the Merged one.

The very low $R^2$ indicate that there are no strong relationships between explicative variables and the uncertainty. Assuming NSO is related with the timing error of the fire detection, results suggest that timing errors are a small part among the total errors of the product found with the current reference data. Since reference data are generated from pairs of satellite images, a relatively large proportion of timing errors may be diluted along the time period between reference image pairs. For example, in a case of image pairs separated by 32 days and a hypothetical product that detects correctly the only pixel burned each day but with a delay of three days, we would still see a relatively high accuracy: 26 pixels correctly classified as burned, three commission errors in the beginning of the time period with reference data, and three omission errors in the end of the time period.

Given the weak TC effect (very low $R^2$) we believe further research is needed to provide insight on the TC effect. Results were also inconclusive for land cover (LC). Even a moderate $R^2$ some land cover types had significant effect although with difficult interpretations. Those significant effects may be caused solely by the directed sample (current results are derived from the data at then study sites). The use of a larger sample derived from a probabilistic sampling should provide more reliable results. Similar results are derived for BIO. It is difficult to compare the importance between some variables, since $R^2$ cannot be compared between qualitative and quantitative variables.

# 6 Conclusion

The methodology to quantify the uncertainty was presented, expressed in probabilistic terms as required by end-users. Regression models were proven to be useful to predict an uncertainty value for each BA product estimate. The uncertainty of the MERIS Pixel product was expressed as the probability of a burned pixel ($Prob_{PB}$). The uncertainty of the MERIS Grid Product was expressed in terms of the standard error of BA proportion (SEp) and was based on the product estimate of BA proportion (EBAp). The 25 % of the true BA proportions felt within the intervals defined by EBAp ± $\hat{S}Ep$ , less than what should be expected for standard errors (68.2 %). The location of the burned detections within a burned mapped patch was found to explain a large part of the uncertainty and error variability in the Pixel Products MERIS, VGT and Merged. The commission errors tended to be slightly related with the confidence level (CL). No clear trends were found between error occurrences and the number of sensor observations (NSO), and the land cover variables (LC, BIO and TC).

The fact that the uncertainty assessment is only a small part of a BA product, no time may be available to calibrate and prepare the uncertainty quantification. Therefore, it would be recommendable to include the uncertainty calibration and quantification within the processing chain.

# 7 References

Burnicki, A.C. (2011). Modeling the Probability of Misclassification in a Map of Land Cover Change. Photogrammetric Engineering & Remote Sensing, 77, 39-49.

Chuvieco, E., Calado, T. & Oliva, P. (2014). ESA CCI ECV Fire Disturbance - Product Specification Document: Fire_cci_Ph2_UAH_D1_2_PSD_v4_3.pdf. www.esa-fire-cci.org

Crosetto, M., Moreno, J.A., & Crippa, B. (2001). Uncertainty propagation in models driven by remotely sensed data. Remote Sensing of Environment, 76, 373-385.

Crosetto, M., & Tarantola, S. (2001). Uncertainty and sensitivity analysis: tools for GIS-based model implementation. International Journal of Geographical Information Systems, 15, 415-437.

Giglio, L., Loboda, T., Roy, D.P., Quayle, B., & Justice, C.O. (2009). An active-fire based burned area mapping algorithm for the MODIS sensor. Remote Sensing of Environment, 113, 408-420.

Giglio, L., Randerson, J., T., van der Werf, G.R., Kasibhatla, P., Collatz, G.J., Morton, D.C., & Defries, R. (2010). Assessing variability and long-term trends in burned area by merging multiple satellite fire products. Biogeosciences Discuss, 7, 1171.

Hastie, T., & Tibshirani, R. (1990). Generalized Additive Models: Chapman & Hall.

JCGM (2008a). Evaluation of measurement data — Guide to the expression of uncertainty in measurement In: Joint Committee for Guides in Metrology

JCGM (2008b). Evaluation of measurement data — Supplement 1 to the "Guide to the expression of uncertainty in measurement" — Propagation of distributions using a Monte Carlo method. In: Joint Committee for Guides in Metrology.

Laris, P.S. (2005). Spatiotemporal problems with detecting and mapping mosaic fire regimes with coarse-resolution satellite data in savanna environments. Remote Sensing of Environment, 99, 412-424.

Nagelkerke, N.J.D. (1991). A note on a general definition of the coefficient of determination. Biometrika, 78, 691-692.

Olson, D.M., Dinerstein, E., Wikramanayake, E.D., Burgess, N.D., Powell, G.V.N., Underwood, E.C., D'Amico, J.A., Itoua, I., Strand, H.E., Morrison, J.C., Loucks, C.J., Allnutt, T.F., Rcketts, T.H., Kura, Y., Lamoreux, J.F., Wettengel, W.W., Hedao, P., & Kassem, K.R. (2001a). Terrestrial Ecoregions of the World: A New Map of Life on Earth BioScience, 51, 933-938.

Olson, D.M., Dinerstein, E., Wikramanayake, E.D., Burgess, N.D., Powell, G.V.N., Underwood, E.C., D'Amico, J.A., Itoua, I., Strand, H.E., Morrison, J.C., Loucks, C.J., Allnutt, T.F., Ricketts, T.H., Kura, Y., Lamoreux, J.F., Wettengel, W.W., Hedao, P., & Kassem, K.R. (2001b). Terrestrial Ecoregions of the World: A New Map of Life on Earth BioScience, 51, 933-938.

Padilla, M., & Chuvieco, E. (2014). Padilla, M., & Chuvieco, E. (2014) ESA CCI ECV Fire Disturbance - Product Validation Report II, Fire_cci_Ph3_UAH_D4_1_2_PVRII_v1_3.pdf, www.esa-fire-cci.org

Padilla, M., Chuvieco, E.Hantson, S., Theis, R., & Snadow, C. (2011). ESA CCI ECV Fire Disturbance - Product Validation and Algorithm Selection Report: Fire_cci_Ph2_UAH_D2_1_PVASR_v2_0.pdf, www.esa-fire-cci.org

Roy, D.P., & Boschetti, L. (2009). Southern Africa validation of the MODIS, L3JRC, and GlobCarbon burned-area products. IEEE Transactions on Geoscience and Remote Sensing, 47, 1032-1044.

Sá, A.C.L., Pereira, J.M.C., & Gardner, R.H. (2007). Analysis of the relationship between spatial pattern and spectral detectability of areas burned in southern Africa using satellite data International Journal of Remote Sensing, 28, 3583-3601.

Silva, J., Sá, A., & Pereira, J.M.C. (2005). Comparison of burned area estimation derived from SPOT-VEGETATION and Landsat ETM+ data in sAfrica: Influencia de spatial pattern and vegetation type. Remote Sensing of Environment, 96, 188-201.

Smith, J.H., Stehman, S.V., Wickham, J.D., & Yang, L. (2003). Effects of landscape characteristics on land-cover class accuracy. Remote Sensing of Environment, 84, 342-349.

Tansey, K., & Bradley, A. (2014). ESA CCI ECV Fire Disturbance - Algorithm Theoretical Basis Document Volume III: Fire_cci_Ph3_UL_D3_6_3_ATBD_III_v2_3.pdf, www.esa-fire-cci.org

van Oort, P.A.J., Bregt, A.K., de Bruin, S., de Wit, A.J.W., & Stein, A. (2004). Spatial variability in classifiaction accuracy of agricultural crops in the Dutch national land-cover database. International Journal of Geographical Information Science, 18, 611-626.

van Oort, P.A.J., Bregt, A.K., de Bruin, S., de Wit, A.J.W., & Stein, A. (2011). Spatial variability in classifiaction accuracy of agricultural crops in the Dutch national land-cover database. International Journal of Geographical Information Science, 18, 611-626.

Wood, S.N. (2006). Generalized Additive Models. An Introduction with R: Chapman and Hall/CRC.

# ANNEX A: Equations fitted to quantify the uncertainty of the Grid and Pixel MERIS products

Table A1: The coefficients of the uncertainty quantification model for the burned classifications of the Merged Pixel product. P-value refers to the significance of the coefficient difference to zero.

| | Coefficient | P-value |
|---|---|---|
| (Intercept) | -1.69 | 3e-109 |
| NEI | 0.03 | 1e-107 |

Table A2: The coefficients of the uncertainty quantification model for the Merged Grid product. P-value refers to the significance of the coefficient difference to zero.

| | Coefficient | P-value |
|---|---|---|
| EBAp | 0.36276 | 2.33e-07 |

# ANNEX B: Relationships between error factors and the errors of the intermediate products

The intermediate product of Merged Product

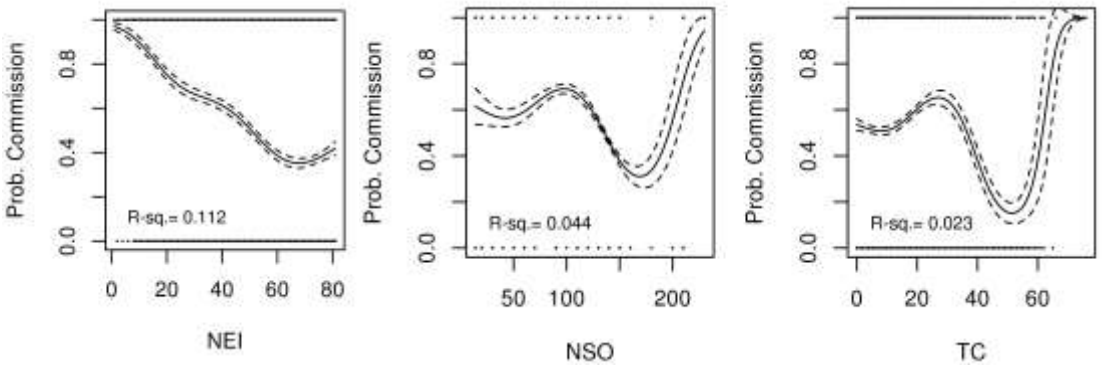


**Figure B1: Scatter plots between the explanatory variables (x-axes) and the commission errors (y-axes; 1 if error and 0 if no-error) for the Pixel Product. The relationship between each variable and the errors, calibrated through GAM, are shown with the expected probability of a commission error (solid line) and its 95% confidence intervals (slashed line). The coefficient of determinations (R-sq.) of each model, adjusted by the residual degrees of freedom, is shown at the bottom-right of the figures.**

**Table B1: Effects of the categorical variables over the commission errors of the Pixel Product. Nagelkerke $R^2$ for the logistic regression models the sign of the coefficient in cases they are significantly different than zero ($\alpha < 0.05$)**

| Variable | Nagelkerke $R^2$ | Signs of the coefficients with significant effect |
|---|---|---|
| BIO | 0.110 | boreal.forest(+); desert(-); temp.savana(-); trop.moist.forest(-); trop.savana(-) |
| LC | 0.121 | broad.everg.(+); clos.needl.(-); openneedl.(+); shrubland(-); spar.veg.(-); water(+) |

**Figure B2: As in Figure B1 but for the omission errors**

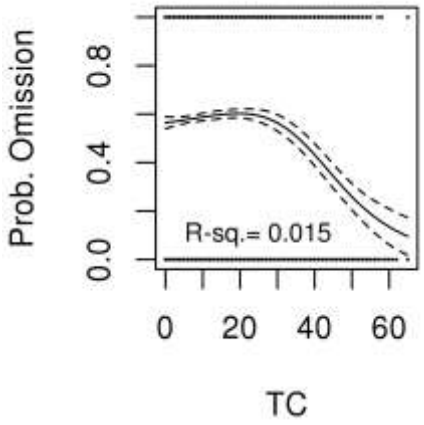


Table B2: As in Table B but for the omission errors

| Variable | Nagelkerke.R.square | Coeficient signs |
|---|---|---|
| BIO | 0.039 | boreal.forest(-); desert(+); medit.forest(+); trop.moist.forest(+); trop.savana(+) |
| LC | 0.047 | agromosaic(+); grass(-); grass& forest(-); opendecid.(+); openneedl.(-) |

The intermediate product of VGT

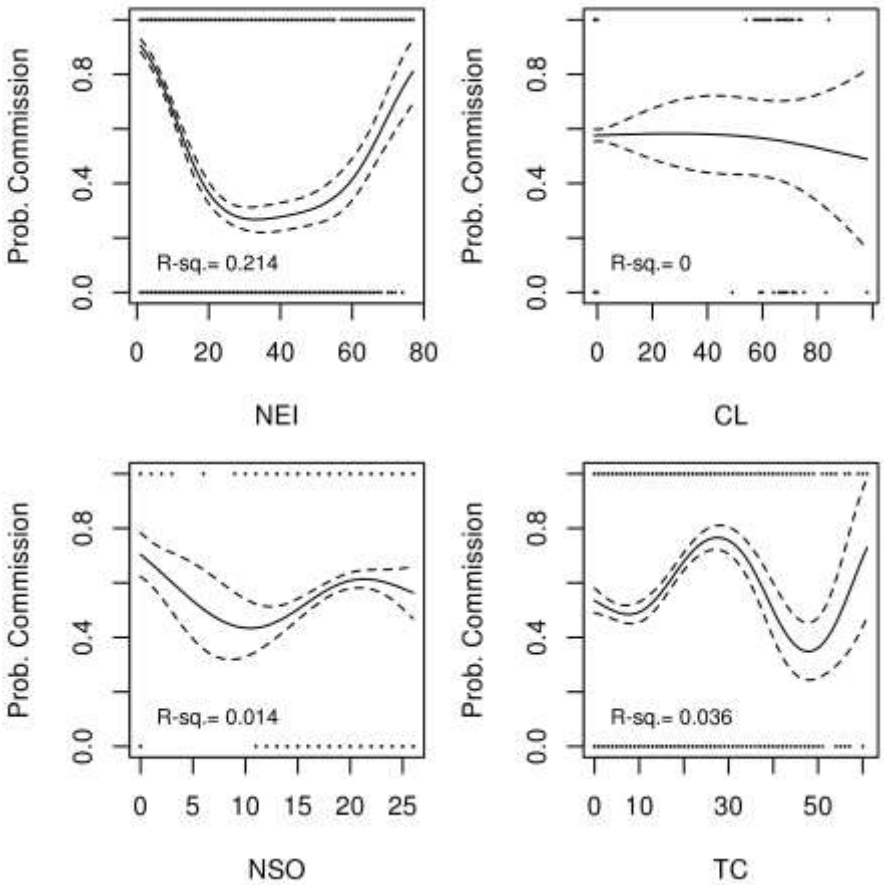


**Figure A3: As in Figure B1 but for the intermediate product of VGT**

**Table A3: As in Table B but for the intermediate product of VGT**

| Variable | Nagelkerke $R^2$ | Signs of the coefficients with significant effect |
|---|---|---|
| BIO | 0.282 | boreal.forest(+); desert(-); temp.savana(-); trop.moist.forest(-); trop.savana(-) |
| LC | 0.242 | grass& forest(+); openneedl.(+); rain.cropl(+); spar.veg.(-); water(+) |

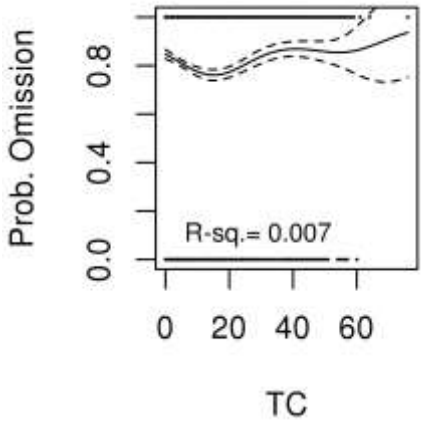


**Figure A4: As in Figure B1 but for the omission errors and the intermediate product of VGT**

**Table A4: As in Table B but for the omission errors and the intermediate product of VGT**

| Variable | Nagelkerke.R.square | Coeficient signs |
|---|---|---|
| BIO | 0.028 | boreal.forest(+); desert(-); temp.savana(-); trop.savana(-) |
| LC | 0.102 | agromosaic(+); bare(-); clos.decid.(+); forest& grass(-); grass(-); opendecid.(+); openneedl.(+); shrubland(+) |